Published in final edited form as:

Biomech Model Mechanobiol. 2014 April ; 13(2): 451–462. doi:10.1007/s10237-013-0508-x.

A TIME-DEPENDENT PHENOMENOLOGICAL MODEL FOR CELL MECHANO-SENSING

Carlos Borau[1], **Roger D. Kamm**[2], and **José Manuel García-Aznar**[1]

Carlos Borau: cborau@unizar.es; Roger D. Kamm: rdkamm@mit.edu; José Manuel García-Aznar: jmgaraz@unizar.es

[1]Aragón Institute of Engineering Research (I3A), Department of Mechanical Engineering, University of Zaragoza Campus Rio Ebro 50018 Zaragoza, SPAIN

[2]Departments of Biological and Mechanical Engineering, Massachusetts Institute of Technology, 77 Massachusetts Avenue, Cambridge, MA 02139-4307, USA

Abstract

Adherent cells normally apply forces as a generic means of sensing and responding to the mechanical nature of their surrounding environment. How these forces vary as a function of the extracellular rigidity is critical to understanding the regulatory functions that drive important phenomena such as wound healing or muscle contraction. In recognition of this fact, experiments have been conducted to understand cell rigidity-sensing properties under known conditions of the extracellular environment, opening new possibilities for modeling this active behaviour. In this work, we provide a physics-based constitutive model taking into account the main structural components of the cell to reproduce its most significant contractile properties such as the traction forces exerted as a function of time and the extracellular stiffness. This model shows how the interplay between the time-dependent response of the acto-myosin contractile system and the elastic response of the cell components determine the mechano-sensing behaviour of single cells.

Keywords

Mechano-sensing; Modeling; Motor activation

1. INTRODUCTION

Currently, there exists much interest in characterizing the mechanical properties of living cells as a material (Kasza et al. 2007). In particular, cells behave completely different when supporting loads (passive) than when exerting forces (active) (Kollmannsberger and Fabry 2011; Ronan et al. 2012; Ujihara et al. 2012). In fact, cells are constantly pulling on the extracellular matrix (ECM) in order to evaluate the mechanical environment and accordingly respond, adjusting their properties. This mechanism that cells use to sense rigidity has been attributed to two main contributions: cytoskeleton contractility and adhesion complexes (Discher et al. 2005). However, recent experimental works have shown the predominant role of cell contractility. In fact, some of these experiments (Fouchard et al. 2011; Mitrossilis et al. 2010; Mitrossilis et al. 2009) suggest that contractility at cell scale due to acto-myosin

Correspondence to: Carlos Borau, cborau@unizar.es.

response to load is the main hypothesis to understand rigidity sensing mechanism. Others, however, have presented strong evidences that the rigidity-sensing mechanism in cell migration is not only locally driven by focal adhesion growth, but also mediated by a larger-scale mechanism originating in the cytoskeleton (Trichet et al. 2012).

Many different experimental (Kobayashi and Sokabe 2010; Trichet et al. 2012; Ghassemi et al. 2012) and computational works (McGarry et al. 2009; Zemel et al. 2010; Vernerey and Farsad 2011) have been developed in order to characterize the mechanical active response of cells under different rigidity conditions of the extracellular environment. In particular, novel experiments using uni-axial loading conditions with a precise control of the mechanical properties of the extracellular environment have been rising. In this sense, Mitrossilis et al (Mitrossilis et al. 2009) have recently developed a single cell traction force experiment with a custom-made parallel microplate setup. In this study, the authors adhere single cells to two parallel glass microplates coated with bronectin. One plate was rigid, whereas the other was flexible and used as a nano-Newton force sensor (i.e., a spring of calibrated stiffness). A computer-controlled detection of the flexible plate deflection allowed quantifying real-time single cell traction forces. Therefore, using this setup they were able to measure the cell response as a function of the plate rigidity. In a first phase, the forces increased at different rates, depending on the plate stiffness. After approximately 10 minutes, the forces saturated reaching a plateau. This plateau force was observed to depend upon the stiffness of the flexible plate as long as the stiffness is less than 60nN/μm. However, at higher stiffness values, the plateau force achieved a maximum value of $\approx$ 300 nN that was independent of the stiffness.

Moreover, using this measurement system is facile to induce a step change in the extracellular stiffness in order to evaluate the viscoelastic response of cell contraction to this change. In fact, recently, several authors carried out this experiment, concluding that contracting cells are able to adapt to the stiffness step change on a short timescale of 10's of seconds, showing practically an instantaneous response (Crow et al. 2012; Mitrossilis et al. 2010).

Collectively, these experiments constitute a set of benchmark data that can be used to validate the predictive potential of models to simulate mechanosensing. The first computational model developed to simulate the mechanosensory role of cells was proposed by Schwarz et al (Schwarz et al. 2006) and was based on a two-spring approach (Fig. 1a). This model is able to predict saturation force phenomena, although the plateau force is independent of extracellular stiffness. Different "three-spring" approaches have been also proposed to model mechanosensing phenomenon (Fig. 1b). In particular, Moreo et al. (Moreo et al. 2008) presented a three-spring model with a linear stiffness-dependent actuator, which was capable of predicting cell contractility in response to changes in extracellular matrix stiffness (Fig. 1c). Their mechanical approach, however was static, whereas real cell contractility is time-dependent as has been extensively exhibited experimentally (Mitrossilis et al. 2009). To overcome this limitation several authors have proposed a different theoretical model based on active matter theory (Zemel et al. 2010; Marcq et al. 2011). Indeed, Zemel et al (Zemel et al. 2010) established a new model in order to understand the stiffness-dependent orientation of stress fibers in adherent cells. Marcq et

al (Marcq et al. 2011) focused their modeling work on the analysis of the temporal cell response to substrate rigidity, but, they did not study the response of their model to sudden changes in substrate rigidity. Recently, Foucard and Vernerey (Foucard and Vernerey 2012) investigated the viscoelastic behavior of stress fibers, but their primarily addressed the dependence of stress fiber elasticity on stretching frequency. Deshpande et al. combined mechanics with time-dependent chemical signaling (Deshpande et al. 2006) in order to predict the role of focal adhesions and stress fiber concentration in the development of force by cells. Finally, Crow and co-workers (Crow et al. 2012) proposed a three-spring model including a dashpot and an independent actuator contracting at a constant velocity (Fig. 1d), although their approach was focused on capturing the instantaneous cell response rather than the long term behavior. Notably, with this scheme the authors were able to adjust a mechanical law to successfully simulate step changes induced in the extracellular rigidity; however, their model is not able to predict temporal saturation of forces under different stiffness. Therefore, to fully predict this benchmark of experiments, we propose a novel one-dimensional constitutive law for cell contractility and force generation, capable of reproducing some important features of cell response to extracellular stiffness.

2. CONSTITUTIVE LAW

In this work, we extend the model proposed by Moreo et al (Moreo et al. 2008) to include rate-dependent effects. The system is similar as in the previous work, consisting on two parallel springs representing the stiffness of the passive mechanical components of the cell and the actin filaments which are, furthermore, in series with the myosin motor contractile system (Fig. 2). This approach was purely mechanical and static, so that the contractile system exerted a specific force depending on the cell strain, and thus depending on the substrate stiffness. However, the time-force evolution, which plays a critical role in cell mechano-sensing, was not taken into account. These rate-dependent or viscous effects have already been included into other models by means of the addition of dashpots, e.g. in the three-spring approach, however, they are not able to simulate all cell responses associated with changes in the extracellular rigidity. Hence, a different approach is here presented incorporating an internal variable that takes into account the kinetics associated to cell molecular motors, in particular, the force saturation due to motor stalling.

2.1 Definition of internal variables

To simulate the cell we consider a one-dimensional mechanical device consisting of two springs and a linear stiffness-dependent actuator f_c (δ_c) (Fig. 2b). The active force of the contractile actuator simulates the force provided by the actin and myosin cross-bridges at the sarcomere level when shortening. In this scheme, the series element K_{act} corresponds to the stiffness of the actin components and the parallel element K_{pas} to the stiffness of different mechanical components of the cells, such as, the membrane, microtubules, cytoplasm and others. In addition, K_{subs} corresponds to the extracellular or substrate stiffness that describes the rigidity associated to the deformed plate used in the mechanosensing experiments (Mitrossilis et al. 2009) presented above.

The temporal response of the cell is characterized by using an internal variable as follows: let [0,T] be the time interval of interest. We consider the internal variable

$$\alpha:[0,T]\rightarrow R$$

and interpret $\alpha(t)$ as the level of motor stalling, that is to say, the ratio of myosin molecules that are stalled, with α =1 meaning that the cell has reached equilibrium (Borau et al. 2012). Therefore, this ratio takes on various values corresponding to the range $0 \leq \alpha(t) \leq 1$.

From a phenomenological point of view we regard motor activation as an internal variable, which is characterized in terms of the history of the cell contraction displacements $\delta_{\text{cell}}(t)$.

2.2 Additive decomposition of the displacement field

The basic assumptions underlying the formulation of this phenomenological model of cell mechanosensing, lead to a set of local governing equations that can be summarized as follows.

From the model depicted in Fig. 2, the compatibility equation in the displacement field can be derived:

$$\delta_{\text{cell}}+\delta_{\text{subs}}=0 \quad \text{(eq.1)}$$

It is assumed that the cell displacement or cell stretching can be decomposed into a contractile and an elastic part. In other words, the total displacement is the sum of the contraction of the acto-myosin system (δ_c) and the extension of the actin filaments (δ_a):

$$\delta_{\text{cell}}=\delta_a+\delta_c \quad \text{(eq.2)}$$

2.3 Cell forces

The force that a cell exerts on the plate or the extracellular substrate (f_{cell}) is defined through the stiffness of the substrate K_{subs} and the variation of the cell height (δ_{cell})

$$f_{\text{cell}}=K_{\text{subs}}\delta_{\text{subs}}=-K_{\text{subs}}\delta_{\text{cell}} \quad \text{(eq.3)}$$

Now the governing equations for the model depicted in Fig. 2 are derived from equilibrium, where the force that the cell exerts can be decomposed into the force exerted by the contractile system and the force borne by the passive matrix of the cell:

$$f_{\text{cell}}=f_c+f_m \quad \text{(eq.4)}$$

where f_m depends on the cell passive stiffness

$$f_m=K_{\text{pas}}\delta_{\text{cell}} \quad \text{(eq.5)}$$

Cell tension is generated by the myosin II molecular motors walking along the actin filaments. The force generated by the activity of myosin causes oppositely orientated actin

filaments to slide relative to one another if they are free to move, or to experience tension if they are not. For simplicity, Moreo et al. (Moreo et al. 2008) assumed the following linear constitutive relationship connecting the contractile acto-myosin force f_c and the relative slippage distance between the actin filaments δ_c, according to the classical Huxley's law:

$$f_c(\delta_c) = \begin{cases} f_{\max}\left(1-\frac{\delta_c}{\delta_1}\right) & if \quad \left(1-\frac{\delta_c}{\delta_1}\right) > 0 \\ 0 & if \quad \left(1-\frac{\delta_c}{\delta_1}\right) < 0 \end{cases} \quad \text{(eq.6)}$$

where f_{max} describes the zero-slippage force and δ_1 is the maximum slippage distance. In the same way that Huxley (Huxley 1957) defined a maximum cross-bridge extension to limit the number of attached motors, we establish a range where the dependence of acto-myosin force on slippage is valid. Hence, for slippages higher than this maximum distance ($\delta_c \geq \delta_1$), the acto-myosin force (f_c) drops to 0. At zero slippage ($\delta_c = 0$), f_c is maximum. With no further assumptions, in this model (Moreo et al. 2008), the mechanical equilibrium is independent of time, and f_c takes a unique value for a given δ_c, which in turn depends on the substrate stiffness, as will be shown below. To account for time-dependent phenomena, Huxley used cross-bridge attachment and detachment rates, as well as transport effects due to relative fiber motion. Here we assume that this time-dependent response is based on the stalling of myosin motors with time. Hence, eq. 6 should be equivalent to the real constitutive equation when the system has reached steady state ($\alpha = 1$); that is to say, when all the motors are actively walking along the actin filaments exerting maximum force. Therefore eq.7 is naturally updated from the previous expression by introducing the fraction of active motors ($\alpha(t)$). In this way, although the linear relationship between f_c and δ_c remains, the force that the acto-myosin actuator is able to exert increases with time, and accordingly with α, as shown in Fig. 3a. The force exerted by the motors and transmitted to the actin filaments can be then expressed as:

$$f_c(\delta_c, \alpha) = K_{\text{act}}\delta_a = \begin{cases} f_{\max}\left(\alpha(t)-\frac{\delta_c}{\delta_1}\right) & if \quad \left(\alpha(t)-\frac{\delta_c}{\delta_1}\right) > 0 \\ 0 & if \quad \left(\alpha(t)-\frac{\delta_c}{\delta_1}\right) \leq 0 \end{cases} \quad \text{(eq.7)}$$

Note that this expression renormalizes both the maximum contraction and maximum force that the AM system is able to do at each time instant (Fig 3.a) and ensures the continuity of the time dependent response as discussed in the next section. This eq. 7 aims to model the contractile activity due to the acto-myosin machinery, nevertheless, the expression could be generalized to incorporate also negative forces (cell pushing the matrix) due to other different mechanisms such as actin polymerization (Mogilner 2009).

By equilibrium of forces, and combining equations 3,4,5 and 6 we can find a direct relationship between the relative displacement of the actin filaments of the acto-myosin contractile system $\delta_c(t)$ and the ratio of active motors $\alpha(t)$ being dependent on extracellular rigidity:

$$\delta_c(t) = \frac{(K_{\text{act}}+K_{\text{pas}}+K_{\text{subs}})\ f_{\max}\delta_1}{(K_{\text{act}}+K_{\text{pas}}+K_{\text{sub}})\ f_{\max} - (K_{\text{pas}}+K_{\text{subs}})\ K_{\text{act}}\delta_1}\alpha(t) \quad \text{(eq.8)}$$

Using the same procedure, the force that a cell transmits to the substrate can be derived as a function of $\alpha(t)$ and K_{subs}:

$$f_{cell}=\alpha(t)f_{max}\frac{\frac{K_{subs}}{K_{act}}}{\left(\frac{K_{subs}}{K_{act}}+\frac{K_{pas}}{K_{act}}\right)\left(1-\frac{f_{max}}{K_{act}\delta_1}\right)-\frac{f_{max}}{K_{act}\delta_1}} \quad \text{(eq.9)}$$

2.4 Time-dependent response

As described in previous works, motors can walk, bind and unbind depending on the forces supported (Guo and Guilford 2006), and during this process, they are able to generate increasing contraction forces in the cell network. Eventually, a mechanical equilibrium is reached due to generalized stalling of the motors. These stalling events may occur for several reasons such as high forces, arrival at barbed ends or blocking due to lack of binding sites. These phenomena and their role in cell mechanosensing were previously explored in (Borau et al. 2012). In that work, using a Brownian dynamics computational model, we found that although the cause for motor stalling depends on the extracellular matrix (ECM) compliance, the number of stalled motors and the stalling evolution with time is practically independent of ECM stiffness. Other previous phenomenological models assumed the relaxation time to be a decreasing function of substrate rigidity (Marcq et al. 2011; Crow et al. 2012). However, this dependency was found to be significant only at very short times. In fact, Crow et al (Crow et al. 2012) showed experimentally that relaxation time ranges between 6.53 s (for null substrate stiffness) and 2.64 s (for infinity rigid substrates). Hence, for the long term response (~1000 s as used in Mitrossilis's experiments), a constant relaxation time gives similar results.

In this work, we propose a general and simplified regulatory rule to define the temporal evolution of motor stalling depending on the force transmitted through the actin filaments (f_c) and independent of substrate rigidity, with the following explicit form:

$$\dot{\alpha}=\frac{g(f_c)}{\mu} \quad \text{(eq.10)}$$

where μ [nN.s] is a viscosity coefficient and $g(f_c)$ is the regulatory function that controls this time evolution, defining the system approach to its maximum force[§]:

$$g(f_c)=f_c^{max}-f_c=f_{max}\left(1-\frac{\delta_c}{\delta_1}\right)-f_{max}\left(\alpha(t)-\frac{\delta_c}{\delta_1}\right)=f_{max}\left(1-\alpha(t)\right) \quad \text{(eq.11)}$$

[§]Different functions may have been use to define $g(f_c)$, always fulfilling the experimental evidences. Here, we chose this function of $g(f_c)$ for simplicity, so that the terms depending on substrate stiffness (δ_c) are cancelled in equation 11. This ensures the continuity when integrating equation 12, even when the substrate stiffness is time-dependent. Furthermore, the resulting exponential function $\alpha(t)$ can be physically interpreted as the motor stalling evolution found in previous studies. Certainly $g(f_c)$ could be revised if f_c was differently defined. In fact, its current definition (equation 7) permits to renormalize both the slippage and the force exerted by the AM system so that its contraction varies in time even for a fixed value of substrate stiffness. In addition, the selection of the current $g(f_c)$ implies a relaxation time independent of substrate stiffness. This assumption is adequate for the long-term response, which is the principal aim of our model (end of footnote).

Combining equations 10 and 11, and defining $\tau = f_{max}/\mu$ as the relaxation time, we obtain the evolution of motor stalling:

$$\dot{\alpha} = \frac{f_{\max}(1-\alpha)}{\mu} = \frac{(1-\alpha)}{\tau} \quad \text{(eq.12)}$$

On physical grounds, we assume as initial condition ($t = 0$) that $\alpha(t) = \alpha_0$ and integrating this equation, we obtain the expression that defines the evolution of $\alpha(t)$

$$\alpha(t) = 1 + (\alpha_0 - 1)e^{\frac{-t}{\tau}} \quad \text{(eq.13)}$$

Using the specific values of the different parameters indicated in Table 1, we compute the temporal evolution of α and the forces generated by the contractile system (f_c) and those transmitted to the substrate (f_{cell}) as a function of the relative slide and time, respectively (Fig. 3a–d). Note that although the relaxation time (τ) is substrate stiffness-independent, the rate of force build-up (dF/dt) is not, capturing the stiffness-dependent instantaneous cell response as shown in next section.

$$\frac{dF}{dt} = \frac{(1-\alpha)}{\tau} f_{\max} \frac{\frac{K_{\text{subs}}}{K_{\text{act}}}}{\left(\frac{K_{\text{subs}}}{K_{\text{act}}} + \frac{K_{\text{pas}}}{K_{\text{act}}}\right)\left(1 - \frac{f_{\max}}{K_{\text{act}}\delta_1}\right) - \frac{f_{\max}}{K_{\text{act}}\delta_1}} \quad \text{(eq.14)}$$

3. RESULTS

3.1 Problem description

A single cell fixed between a rigid and a flexible plate is simulated in order to reproduce the experimental setup designed by Mitrossilis et al.(Mitrossilis et al. 2009) and used by different authors (Webster et al. 2011; Crow et al. 2012) to evaluate cell mechano-sensing properties (Fig. 2a). In this setup, the cell pulls on the two parallel plates while the plate deflection is measured. By using a double feedback loop which independently regulates spring and cell lengths to maintain cell-spring contact in a fixed position, they obtain the temporal cell response for different external rigidities.

A simplified one-dimensional problem is defined to understand contractility and force generation due to cell response under different extracellular rigidities (Fig. 2b). Two main conditions are simulated. Firstly, we evaluate the temporal evolution of cell contractility and force generation under a wide range of extracellular rigidity values. Secondly, we compute the cellular time-response under step-changes of the extracellular stiffness.

3.2 Cell contraction and force generation under different extracellular stiffnesses

The temporal evolution of force generation, which depends on the extracellular rigidity, is shown in Fig. 3d and Fig. 4a. In the former, and according to eq. 9, force develops following the evolution of motor activation. The maximum value achieved (the plateau force, f_p) depends on the substrate stiffness (K_{subs})(Fig. 4b). Actually, the model predictions are similar to experimental data from (Mitrossilis et al. 2009). At a given time, the force

increases with stiffness, abruptly for low stiffness and smoothly for higher ones (Fig. 4a). Qualitatively similar results were found experimentally, measuring the cell stress exerted on micropillars of different stiffness. (Trichet et al. 2012). Taking the force at t=1200 seconds as the plateau force and plotting it against substrate stiffness, we find that for K_{subs} < 100 nN/μm, f_p rapidly increases with stiffness, saturating for higher rigidities, in good agreement with experiments (Mitrossilis et al. 2009). In fact, both in the model and experiments, f_p is proportional to K_{subs} in compliant substrates (~ $K_{subs}^{0.87}$ and ~ $K_{subs}^{0.94}$ respectively). In addition, other authors found this initial linear relationship (~ $K_{subs}^{0.93}$) (Trichet et al. 2012), although their study only took into account substrate stiffness up to 80 nN/ μm (Fig. 4b). The rate of force build-up (*dF/dt*, slope of the force curve) increases quickly and proportionally to the stiffness at first, and slows down as the force approaches the maximum plateau (~300 nN (Mitrossilis et al. 2009)). In relation with the substrate stiffness and measuring *dF/dt* in the first phase of contraction (t<100 s), the rate of force build-up strongly increases for compliant substrates and presents slight changes for stiffer ones (Fig. 5a), similarly to recent experimental findings (Mitrossilis et al. 2009; Mitrossilis et al. 2010; Trichet et al. 2012). Note that in this last work (Trichet et al. 2012), as in the measurement of the plateau force, only the initial linear regime was observed since their study was focused on compliant substrates.

The speed of shortening (v_{cell}) is easily derived from the rate of force build-up as $v_{cell}=\frac{1}{K_{subs}}\frac{dF}{dt}$. The cell shortening is faster for compliant substrates, whereas stiffer substrates, which resist the contraction, lead to very low velocities for K_{subs} >1000 nN/μm. Fig. 5b shows $1/v_{cell}$ as a function of K_{subs}, both for the model and experiments (Mitrossilis et al. 2009). Mechanical power ($P = f_{cell}\, v_{cell}$) is also computed, presenting a bi-phasic behaviour with the load and showing a peak at ~40% of the maximum generated force, following the classical behavior observed in muscles and recently found in myoblasts (Mitrossilis et al. 2009) due to acto-myosin contraction (Fig. 5c).

3.3 Simulating step changes in extracellular stiffness

In these simulations we evaluate the cell response to step-changes in substrate stiffness with a period of 20 seconds (Fig. 6a top plot), following the experiments carried out by Crow et al. and Webster et al. (Crow et al. 2012; Webster et al. 2011) and of 100 seconds (Fig. 6b top plot), to study the long-term response and compare the results with Mitrossilis et al. data (Mitrossilis et al. 2010). Specifically, K_{subs} is first varied from 10 to 100 nN/μm in a first case, and then from an extremely low value (~0) to an extremely high one (∞) with a period of 20 seconds (Fig. 6a,b) reproducing the experiments of the aforementioned authors (Crow et al. 2012; Webster et al. 2011; Mitrossilis et al. 2010). In both cases, the force generated increases faster (higher slope) when the stiffness is higher (since *dF/dt* increases with K_{subs}) (Fig. 6a,b middle plots) in good agreement with the simulated experiments (Crow et al. 2012; Webster et al. 2011; Mitrossilis et al. 2010). The cell height, however, decreases faster for compliant substrates (Fig. 6a,b bottom plots). The general trend is clearly seen in the cases with extreme values of substrate stiffness. When $K_{subs} \sim \infty$ the force increases very fast (Fig. 6a middle plot), especially during the first seconds when the activation of motors is in its early phase, whereas the cell height remains constant (Fig. 6b bottom plot). In contrast,

when $K_{subs} \sim 0$, the rate of force build-up is near zero but cell height rapidly decreases (Fig. 6b bottom plot). For higher periods of stiffness step change (Fig. 6c), the system behaves similarly but the effect of substrate stiffness on the cell force variation is less relevant as time increases due to the saturation of α. The motor stalling determines the time at which the system reaches equilibrium, however, the force attained at that point depends on the load-history. For this reason, in the case with stiffness step variations from ~0 to ~∞ (Fig. 6c), the plateau force after 500 seconds is below 200 nN, much lower than the value that would correspond to an infinitely rigid substrate (~ 300 nN). Logically the cell contraction is higher than in previous cases due to the long periods of low stiffness. Certainly, the motor stalling could also depend on substrate stiffness due, for instance, to morphology changes of the intracellular network. This could affect the force evolution after each step change, however, it has been reported that although the reasons for motor stalling depend on external stiffness (higher percentage of motors get stalled by forces for stiffer substrates whereas higher percentage of motors get stalled by blocking phenomena if softer substrates), the temporal evolution of stalling remains practically unchanged (Borau et al. 2012).

4. PARAMETER SENSITIVITY ANALYSIS

In order to find which parameters most strongly influence cell rigidity-sensing, a sensitivity analysis is performed. For this analysis, the substrate stiffness is held constant (K_{subs} =100 nN/μm).

The definition of the internal variable that describes the motor stalling evolution (a) is the key for all the time-dependent processes simulated in this model. Thus, a proper understanding of the effects of the involved parameters is needed. The global parameter controlling the time evolution of α is the relaxation time (τ), which determines how fast the stalling events reach saturation and specifically the rising of force with time (dF/dt). Fig. 7a shows how a plateaus faster for lower values of τ. However, τ is not a free parameter, since it depends on μ and f_{max} (eq.12). While μ only affects a, f_{max} affects the mechanical equilibrium, therefore altering the magnitude of the exerted forces (f_{cell}). Fig. 7b shows how the plateau force adjusts due to variations of f_{max}, while the time-evolution remains unchanged. This happens because μ is varied in the same proportion as f_{max} thus leading to a constant relaxation time. If however, f_{max} is varied alone (Fig. 7c), both the plateu force and the relaxation time are affected. High values of f_{max} lead to higher forces, which are, furthermore, attained faster. On the other hand, μ is a parameter only affecting time evolution (Fig. 7d). Hence, changes in μ are equivalent to changes in τ (Fig. 7a).

The purely mechanical components of the cell (K_{pas}, K_{act}) do play an important role in the mechanical equilibrium. The actin stiffness (K_{act}) appears to be the more relevant component in the mechanical system. Therefore, changing its value, leads to substantial changes in the plateau force (Fig. 8a). As shown in Fig. 2, this component is in series with the AM system. Thus, increasing the actin stiffness leads to lower values of δ_c, which in turn increases the cell force (eqs.4 and 6). However, bigger changes of K_{pas} are needed to be reflected in f_{cell} (Fig. 8b). Actually, these changes in the plateau force are only noticeable when K_{pas} has similar or greater values than K_{act}. This is confirmed in Fig. 8c, where both parameters are varied together obtaining similar results to Fig. 8a, where only K_{act} changes.

Moreover, we explore the effects of the slippage distance parameter δ_1. It is important to note that this parameter is independent of the cell length (L_c). Hence, L_c does not affect the results as long as remains constant. However, higher values of slippage, lead to δ_1 higher forces and higher deformability of the cell as shown in Fig. 9. Other authors have taken this value as infinity (Marcq et al. 2011), which is equivalent to consider a constant force of the AM system, independent of substrate stiffness and other parameters. This allows capturing the force-stiffness linearity only for very compliant substrates, whereas our approach is able to extend the linear regime to experimental ranges, as will be discussed subsequently.

5. DISCUSSION

To adhere and migrate, cells generate forces through the cytoskeleton that are transmitted to the surrounding matrix. The ways that cells exert these forces are dependent on the properties of the surrounding extracellular matrix, being rigidity one of the most studied features due to its implications in numerous aspects of cell behavior and function (Zemel et al. 2011). Indeed, Zemel et al. have reviewed theoretical and experimental studies of the physical consequences of cellular forces, generated by acto-myosin contractility, including its role in cell morphology, stress-fiber formation and alignment and the elastic properties of cells. Apart from the various specific force generating or responsive functions that cells perform (e.g., wound healing, remodeling of the extracellular matrix or muscle contraction), cells also apply forces as a generic means of sensing and responding to the mechanical nature of their environment. This mechanosensing mechanism has been hypothesized in theoretical and computational models to explain cell organization (Bischofs and Schwarz 2003), collective (Moreo et al. 2008), and individual 2D (Trichet et al. 2012) cell migration and 3D cell migration (Borau et al. 2011). These and other mechanisms have been proposed from a molecular point of view, as a portion of one cell (Yamaoka et al. 2012; Borau et al. 2012; Wang and Wolynes 2012; Soares e Silva et al. 2011), to macroscopic constitutive laws of the whole cell (Crow et al. 2012; Moreo et al. 2008) or from purely mechanical models to multiphysics models (Besser and Schwarz 2010; Taber et al. 2011). In this work, we propose a macroscopic phenomenological one-dimensional constitutive law to model cell rigidity sensing based on a purely mechanistic approach. Despite its simplicity, the model is able to successfully simulate multiple rigidity-sensing conditions and its results are in good correspondence with experiments. Three main features distinguish the present model from previous ones: macroscopic force generation, time dependent response and a one-dimensional structure approach.

Firstly, we use a three-spring configuration with a length-actuator (linearly dependent on the relative displacement). Further simplifications of this system produce similar mechanical responses as in the work from (Marcq et al. 2011), but diminish the predictive potential of the model in some aspects as discussed below. In fact, in the absence of external loads such as localized forces or pre-stressed substrates, $\alpha(t) - \delta_c/\delta_1$ is always ≥ 0 in eq.7. Thus, the second condition in equation 7 would not be required to reproduce the experiments here presented, and the whole construct could be simplified to a single pre-stressed spring whose equilibrium length is brought to zero through a decay clock (α). Nevertheless, this three-spring configuration allows us to distinguish between active and passive responses of the cell. For example, introducing eq. 13 in eq. 9 leads to a cell force evolution qualitatively

similar to that proposed by Marcq et al. 2011, although important differences can be identified. Mechanistically, the addition of the series spring (K_{act}) with the acto-myosin actuator, as well as the dependence of f_c with δ_c, captures the linearity of f_{cell} with respect to substrate stiffness (K_{subs}) for compliant substrates, and its saturation for higher rigidities. In Marcq's model, where a constant contractile force is applied in parallel with the cell stiffness, the linearity of the transmitted (traction) force is only obtained when substrate stiffness is much lower than cell stiffness ($k_{ext} \ll k_C$ using his notation). In our model, however, this linearity extends up to 100 nN/μm as found in experiments (Mitrossilis et al. 2009). This occurs due to the combination of the K_{act} spring with a force indirectly depending on stiffness (f_c). If this force was considered constant (as in Marcq's model and equivalent to $\delta_1 \rightarrow \infty$), the effect of the K_{act} spring would be cancelled and equation 9 would be simplified to $f_{cell} = \alpha(t)\, f_{max}\, (K_{subs}/(K_{subs} + K_{pas}))$, thus presenting the aforementioned limitations. In addition, relative values of K_{act} and K_{pas} are not arbitrary (Schafer and Radmacher 2005; Lim et al. 2006) and their independent role can be evaluated as we have shown in Fig. 8. In fact, the relation between both values is really relevant, regulating the cell response under different mechanical conditions. This approach may allow us in the future to simulate more complex phenomena such as stress-fiber rigidization, network disruption etc.

Secondly, time-dependent response has been normally considered due to the viscoelasticity of the membrane or to some cytoskeleton components and have been modeled by means of the addition of dashpots (Crow et al. 2012). However, these models are not able to predict simultaneously two distinct experimental phenomena: immediate cell response to rigidity step changes and cell saturation for high rigidities of the substrate. It is required then to model additional effects, such as the dynamics of myosin motors which introduce, furthermore, a physical meaning to the time-dependent response. This fact is in concordance with the hypothesis of active matter theory proposed by several authors (Marcq et al. 2011; Zemel et al. 2010) and has been also tested with a particle-based Brownian dynamics computational model (Borau et al. 2012). In fact, in that model, molecular motors are proposed as one possible mechanism of cell mechanosensing and their dynamics are found to be crucial for the time-dependent force evolution. Other models, however, rather than a mechanical phenomenon, attribute the temporal response to a chemical decaying signal (eg. concentration of Ca^{2+}) that triggers actin polymerization or myosin phosphorylation (Deshpande et al. 2006), obtaining similar trends for force evolution and saturation depending on substrate stiffness. The model here presented incorporates, through the internal variable α, the motor stalling time-evolution, assuming a single decay law. Saturation is achieved when most of the motors become stalled, not being able of exerting higher forces. Similar relaxation laws have been proposed by other authors (Crow et al. 2012; Marcq et al. 2011), although these other works assume relaxation time to be a decreasing function of substrate rigidity. However, this dependence was found to be not significant for long term responses (e.g. only varied from 6.53 s. to 2.64 s for zero and infinite substrate rigidities respectively τ (Crow et al. 2012)). Based on these experimental results and our previous computational work (Borau et al. 2012), we assumed the relaxation time to be independent of substrate stiffness, ensuring the continuity of the motor stalling function (α). Despite this simplification, we are able to achieve good predictions of force

evolution (f_{cell} (t)) and saturation (f_p), quantitatively similar to those found by (Mitrossilis et al. 2009; Mitrossilis et al. 2010) and qualitatively comparable to those found by (Crow et al. 2012; Trichet et al. 2012), which used different time or substrate stiffness magnitude to perform their experiments. In fact, although the relaxation time is independent of K_{subs}, the rate of force build-up (dF/dt) is not (equation 14), permitting to capture the stiffness-dependent instantaneous cell response. As in these experiments, the force develops and saturates at ~300 nN after 1200 seconds (Fig. 3d). In addition, plateau force barely changes for substrate stiffness higher than 100 nN/μm (Fig. 4b) (Mitrossilis et al. 2009). In our model force evolution is mainly exponential according to the motor stalling function (α) which is in agreement with previous computational results (Borau et al. 2012), however, in experiments (Mitrossilis et al. 2009) this evolution presents a biphasic behavior with a linear initial regime of about 600 seconds, followed by a saturation phase. This difference suggests that although myosin motor dynamics may be important, there likely exist other mechanisms, such as bio-chemical signals, that may also regulate rigidity sensing. Nevertheless, the model is able to capture some time-dependent cell responses such as the rate of force build-up (dF/dt) and the contraction speed (v_{cell}) observed in the experiments developed by (Mitrossilis et al. 2009; Mitrossilis et al. 2010; Trichet et al. 2012). Due to the distinct evolution pattern discussed above, the values of these variables differ from experiments, although they are in the same order of magnitude: maximum dF/dt ~1 nN/s in the model compared with ~0.4 nN/s in the experiments (Mitrossilis et al. 2009), and maximum v_{cell} ~0.045 μm/s (~22 s/μm) compared with ~0.014 μm/s (~70 s/μm) (Mitrossilis et al. 2009) (Fig. 5a,b). Interestingly, in spite of these differences, mechanical power (P) presents a biphasic behavior attaining a peak at ~40% of the maximum load, similar to ~30% found experimentally (Fig. 5c) (Mitrossilis et al. 2009). In addition, the model was tested against periodic step changes in substrate stiffness. Specifically we changed stiffness from 10 to 100 nN/μm and from ~0 to ~∞, and we used a period of 20 seconds in a total of 100 seconds (Fig. 6a,b top plot), following the experiments carried out by Crow et al. (Crow et al. 2012; Webster et al. 2011) and a period of 100 seconds in a total of 500 seconds (Fig. 6c top plot), to study longer time response as Mitrossilis et al. (Mitrossilis et al. 2010). Due to the evolution of motor stalling, for shorter times the response is mainly linear, and the stiffness step changes lead to periodic stretches which switch the slope of force build-up. On the other hand, for longer period and simulated time, the effect of substrate stiffness is less relevant as time advances due to the saturation of α. The motor stalling determines the time at which the force exerted by the cell reaches equilibrium, however, this force depends on the load-history. For this reason, when periodically varying the substrate stiffness from ~0 to ~∞ (Fig. 6c) every 100 seconds during 500 seconds, the plateau force is below 200 nN, much lower than the value that would correspond to an infinitely rigid substrate (~ 300 nN). This, again, strengths the idea that there might exist additional mechanisms that permit to keep cell response mainly linear even for the long-term, but reaching plateau afterwards. Note that this could be reproduced in our model by using a high value of τ (to obtain linear-like response for longer times) together with some kind of limiting mechanism that didn't allow the system to increase the force beyond a specific limit (the plateau force). Up to our knowledge, the reasons for this cell behavior are still unknown, so further experiments would be needed to investigate such mechanisms.

Thirdly, the proposed model focuses only on a 1D approach, when the series of experiments simulated are mainly 2D or even 3D (Mitrossilis et al. 2009; Crow et al. 2012; Mitrossilis et al. 2010). Although the experiments focused on the vertical response, cells spread horizontally during contraction, changing from a convex to a concave curvature in the borders and increasing the contact area and changing the load distribution. Obviously, in vivo cell response involves many other factors and complex mechanisms, however, the accuracy obtained in the numerical results suggests that a one-dimensional approach is adequate to model this problem, at least for the simple scheme proposed in the experiments.

Certainly, this model is a first and simple approximation to predict macroscopic active behaviour of the cell as a whole and, although additional effects could be easily incorporated (such as large strains, cytoskeletal remodeling or coupled mechano-chemical analysis), it could serve as a potential guide for experiments which could furthermore be used to test the model. In addition, this model can be suitable to simulate cell migration, since it is hypothesized that cells tend to sense the rigidity of the ECM to regulate their migration direction. In fact, a non-time dependent version of this model was previously used to simulate cell migration in 3D (Borau et al. 2011). Hence, the implementation of this theory in combination with models of cell migration would provide a strong impetus for the development of future models with applications in wound healing, tissue engineering and cancer metastasis.

Acknowledgments

This research was supported by the European Research Council (ERC) through project ERC-2012-StG 306751, the Spanish Ministry of Science and Innovation (DPI 2009-14115-CO3-01), the FPI grant (BES-2010-029927) and the Singapore-MIT Alliance for Research and Technology (SMART).

References

Besser A, Schwarz US. Hysteresis in the cell response to time-dependent substrate stiffness. Biophys J. 2010; 99 (1):L10–12.10.1016/j.bpj.2010.04.008 [PubMed: 20655823]

Bischofs IB, Schwarz US. Cell organization in soft media due to active mechanosensing. Proc Natl Acad Sci U S A. 2003; 100 (16):9274–9279. [PubMed: 12883003]

Borau C, Kamm RD, García-Aznar JM. Mechano-sensing and cell migration: a 3D model approach. Physical Biology. 2011; 8 (6):066008. [PubMed: 22120116]

Borau C, Kim T, Bidone T, Kamm RD, García-Aznar JM. Dynamic Mechanisms of Cell Rigidity Sensing: Insights from a Computational Model of Actomyosin Networks. Plos One. 2012

Crow A, Webster KD, Hohlfeld E, Ng WP, Geissler P, Fletcher DA. Contractile equilibration of single cells to step changes in extracellular stiffness. Biophys J. 2012; 102 (3):443–451.10.1016/j.bpj.2011.11.4020 [PubMed: 22325266]

Deshpande VS, McMeeking RM, Evans AG. A bio-chemo-mechanical model for cell contractility. P Natl Acad Sci USA. 2006; 103 (38):14015–14020.

Discher DE, Janmey P, Wang YL. Tissue cells feel and respond to the stiffness of their substrate. Science. 2005; 310 (5751):1139–1143. [PubMed: 16293750]

Foucard L, Vernerey FJ. A thermodynamical model for stress-fiber organization in contractile cells. Appl Phys Lett. 2012; 100 (1):13702–137024.10.1063/1.3673551 [PubMed: 22271931]

Fouchard J, Mitrossilis D, Asnacios A. Acto-myosin based response to stiffness and rigidity sensing. Cell Adh Migr. 2011; 5 (1):16–19.10.4161/cam.5.1.13281 [PubMed: 20818154]

Ghassemi S, Meacci G, Liu S, Gondarenko AA, Mathur A, Roca-Cusachs P, Sheetz MP, Hone J. Cells test substrate rigidity by local contractions on submicrometer pillars. Proc Natl Acad Sci U S A. 2012; 109 (14):5328–5333.10.1073/pnas.1119886109 [PubMed: 22431603]

Guo B, Guilford WH. Mechanics of actomyosin bonds in different nucleotide states are tuned to muscle contraction. Proc Natl Acad Sci U S A. 2006; 103 (26):9844–9849. [PubMed: 16785439]

Huxley AF. Muscle structure and theories of contraction. Prog Biophys Biophys Chem. 1957; 7:255–318. [PubMed: 13485191]

Kasza KE, Rowat AC, Liu J, Angelini TE, Brangwynne CP, Koenderink GH, Weitz DA. The cell as a material. Current Opinion in Cell Biology. 2007; 19 (1):101–107.10.1016/j.ceb.2006.12.002 [PubMed: 17174543]

Kobayashi T, Sokabe M. Sensing substrate rigidity by mechanosensitive ion channels with stress fibers and focal adhesions. Curr Opin Cell Biol. 2010; 22 (5):669–676.10.1016/j.ceb.2010.08.023 [PubMed: 20850289]

Kollmannsberger P, Fabry B. Linear and Nonlinear Rheology of Living Cells. Annual Review of Materials Research. 2011; 41 (1):75–97.10.1146/annurev-matsci-062910-100351

Lim CT, Zhou EH, Quek ST. Mechanical models for living cells - A review. J Biomech. 2006; 39 (2): 195–216.10.1016/j.jbiomech.2004.12.008 [PubMed: 16321622]

Marcq P, Yoshinaga N, Prost J. Rigidity sensing explained by active matter theory. Biophys J. 2011; 101 (6):L33–35.10.1016/j.bpj.2011.08.023 [PubMed: 21943439]

McGarry JP, Fu J, Yang MT, Chen CS, McMeeking RM, Evans AG, Deshpande VS. Simulation of the contractile response of cells on an array of micro-posts. Philos T R Soc A. 2009; 367 (1902):3477–3497.

Mitrossilis D, Fouchard J, Guiroy A, Desprat N, Rodriguez N, Fabry B, Asnacios A. Single-cell response to stiffness exhibits muscle-like behavior. Proc Natl Acad Sci U S A. 2009; 106 (43): 18243–18248. [PubMed: 19805036]

Mitrossilis D, Fouchard J, Pereira D, Postic F, Richert A, Saint-Jean M, Asnacios A. Real-time single-cell response to stiffness. Proc Natl Acad Sci U S A. 2010; 107 (38):16518–16523. [PubMed: 20823257]

Mogilner A. Mathematics of cell motility: have we got its number? J Math Biol. 2009; 58 (1–2):105–134.10.1007/s00285-008-0182-2 [PubMed: 18461331]

Moreo P, Garcia-Aznar JM, Doblare M. Modeling mechanosensing and its effect on the migration and proliferation of adherent cells. Acta Biomater. 2008; 4 (3):613–621. [PubMed: 18180207]

Ronan W, Deshpande VS, McMeeking RM, McGarry JP. Numerical investigation of the active role of the actin cytoskeleton in the compression resistance of cells. J Mech Behav Biomed Mater. 2012; 14C:143–157.10.1016/j.jmbbm.2012.05.016 [PubMed: 23026692]

Schafer A, Radmacher M. Influence of myosin II activity on stiffness of fibroblast cells. Acta Biomater. 2005; 1 (3):273–280. [PubMed: 16701806]

Schwarz US, Erdmann T, Bischofs IB. Focal adhesions as mechanosensors: The two-spring model. Biosystems. 2006; 83 (2–3):225–232. [PubMed: 16236431]

Soares e Silva M, Depken M, Stuhrmann B, Korsten M, MacKintosh FC, Koenderink GH. Active multistage coarsening of actin networks driven by myosin motors. Proc Natl Acad Sci U S A. 2011; 108 (23):9408–9413.10.1073/pnas.1016616108 [PubMed: 21593409]

Taber LA, Shi Y, Yang L, Bayly PV. A Poroelastic Model for Cell Crawling Including Mechanical Coupling between Cytoskeletal Contraction and Actin Polymerization. J Mech Mater Struct. 2011; 6 (1–4):569–589.10.2140/jomms.2011.6.569 [PubMed: 21765817]

Trichet L, Le Digabel J, Hawkins RJ, Vedula SR, Gupta M, Ribrault C, Hersen P, Voituriez R, Ladoux B. Evidence of a large-scale mechanosensing mechanism for cellular adaptation to substrate stiffness. Proc Natl Acad Sci U S A. 2012; 109 (18):6933–6938.10.1073/pnas.1117810109 [PubMed: 22509005]

Ujihara Y, Nakamura M, Miyazaki H, Wada S. Contribution of actin filaments to the global compressive properties of fibroblasts. J Mech Behav Biomed Mater. 2012; 14C:192–198.10.1016/j.jmbbm.2012.05.006 [PubMed: 23026698]

Vernerey FJ, Farsad M. A constrained mixture approach to mechano-sensing and force generation in contractile cells. J Mech Behav Biomed Mater. 2011; 4 (8):1683–1699.10.1016/j.jmbbm.2011.05.022 [PubMed: 22098869]

Wang S, Wolynes PG. Active contractility in actomyosin networks. Proc Natl Acad Sci U S A. 2012; 109 (17):6446–6451.10.1073/pnas.1204205109 [PubMed: 22493220]

Webster KD, Crow A, Fletcher DA. An AFM-Based Stiffness Clamp for Dynamic Control of Rigidity. PLoS One. 2011; 6 (3):e17807. [PubMed: 21408137]

Yamaoka H, Matsushita S, Shimada Y, Adachi T. Multiscale modeling and mechanics of filamentous actin cytoskeleton. Biomech Model Mechanobiol. 2012; 11 (3–4):291–302.10.1007/s10237-011-0317-z [PubMed: 21614531]

Zemel A, De R, Safran SA. Mechanical consequences of cellular force generation. Curr Opin Solid St M. 2011; 15 (5):169–176.10.1016/j.cossms.2011.04.001

Zemel A, Rehfeldt F, Brown AEX, Discher DE, Safran SA. Optimal matrix rigidity for stress-fibre polarization in stem cells. Nat Phys. 2010; 6 (6):468–473. [PubMed: 20563235]

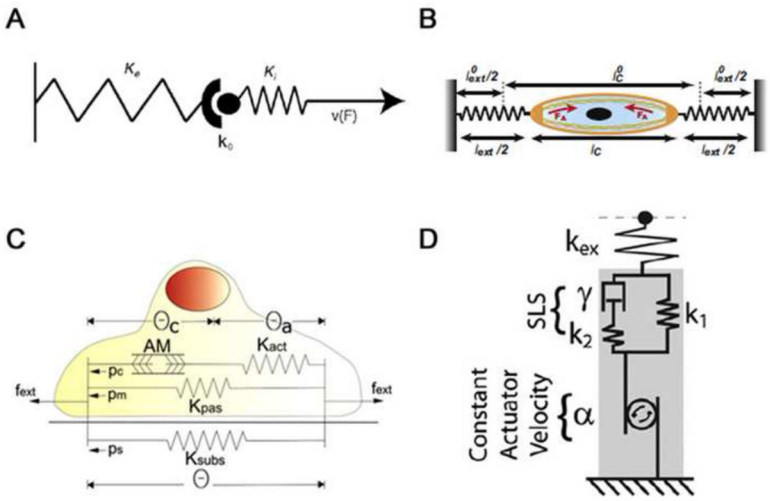

Fig. 1.

Constitutive mechanical models to describe the contractile cell response: (a) the two-spring approach (Schwarz et al., 2006), (b) active matter theory (Marcq et al., 2011), (c) the three-spring approach (Moreo et al., 2008) and (d) the three-spring and a dashpot approach (Crow et al., 2012).

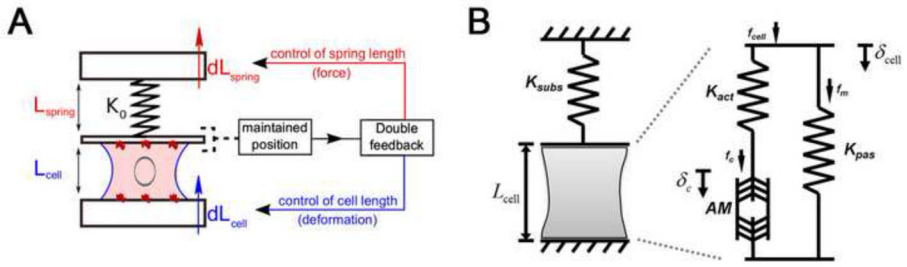

Fig. 2.

System schemes for measuring cell mechanosensing properties. (a) Experimental setup used by (Mitrossilis et al., 2009) to measure the effect of substrate rigidity on cell forces (reproduced with permission from Mitrossilis et al.). They decouple probe elongation (i.e., force) from cell contraction using a double feedback loop which independently regulates spring and cell lengths to maintain cell-spring contact in a fixed position. In this way, the setup acts as if the cell was compressing a spring of stiffness K_0 (dL_{spring} /dL_{cell}), permitting the study of a wide range of rigidities with a single probe of stiffness K_0. (b) Model scheme used in this work to investigate stiffness-dependent cell response. In similar fashion to the experimental setup, the substrate stiffness is represented by a single spring (K_{subs}). The cell body is modeled as two parallel springs, one of them in series with a contractile actuator. K_{pas} represents the passive stiffness of different mechanical components of the cell (e.g. microtubules, membrane, cytoplasm), whereas K_{act} stands for the rigidity of the actin filaments. The acto-myosin system (AM) is then placed in series, contracting the cell body by stretching the actin and compressing the passive components.

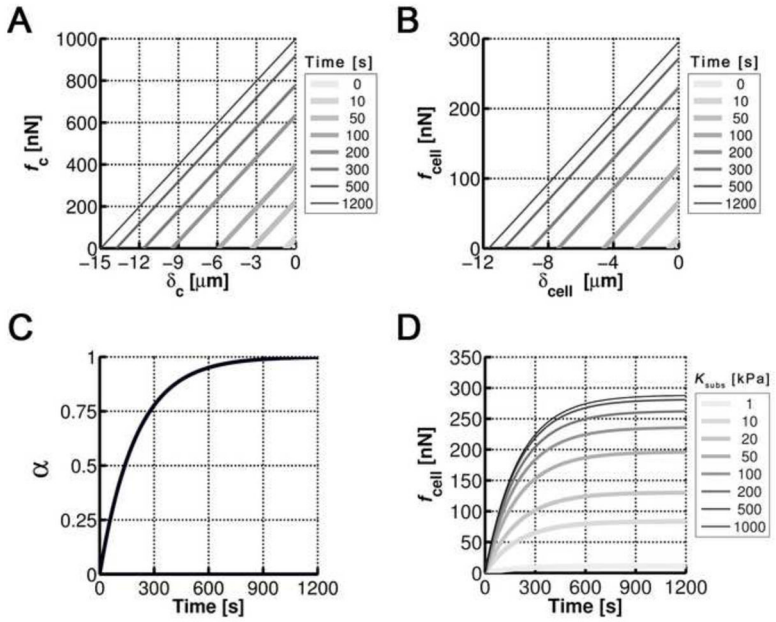

Fig. 3.

(a) Force generated by the contractile system (f_c) as a function of the relative slippage distance between the actin filaments (δ_c) at different times. Longer δ_c leads to lower forces. At a given slippage, the force increases with time. (b) Force of the cell transmitted to the ECM as a function of cell contraction (δ_{cell}) at different times. Longer δ_{cell} leads to lower forces. At a given cell contraction, the force increases with time. (c) Fraction of active motors vs. time. The activity of motors increases with time following an exponential law until saturation. (d) Force evolution for different substrate stiffness. The force increases with time until saturation, at a faster rate for stiffer substrates. The saturation magnitude depends on substrate stiffness, reaching a maximum value of ~300 nN as found experimentally in (Mitrossilis et al. 2009).

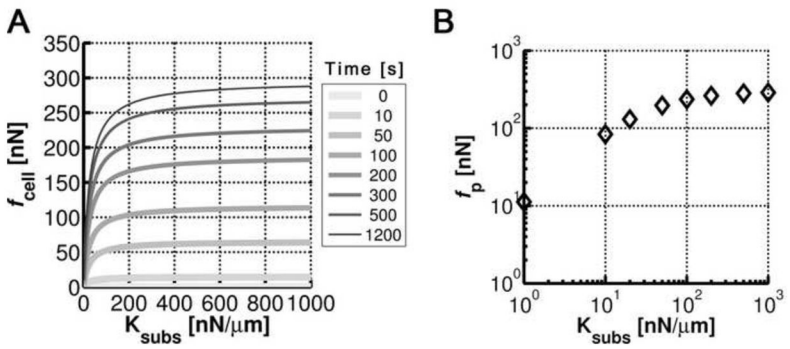

Fig. 4.

(a) Cell force as a function of substrate stiffness for different times. The force increases exponentially at low stiffness, and saturates (plateau force) for higher ones. The force increases with time for all the stiffness due to the growing motor activation. (b) Saturation or plateau force (f_p) as a function of substrate stiffness in log-log scale. f_p, in other words f_{cell} measured at t=1200 s, increases proportionally to K_{subs} ($f_p \sim K_{subs}^{0.87}$) for softer substrates, in similar fashion to the experimental findings from (Mitrossilis et al. 2009) ($f_p \sim K_{subs}^{0.94}$, exp 1 in the legend), and (Trichet et al. 2012)($f_p \sim K_{subs}^{0.93}$, exp 2), and saturates for stiffer ones as in (Mitrossilis et al. 2009).

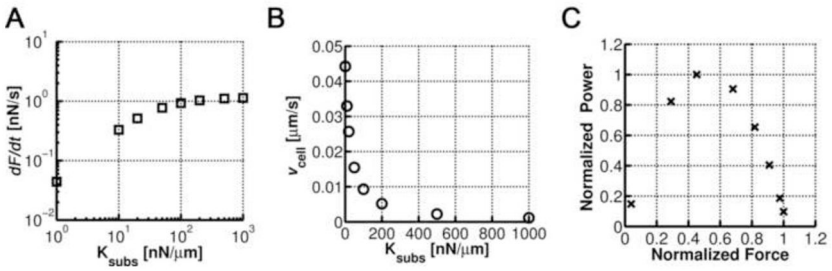

Fig. 5.

(a) Initial rate of force build-up (*dF/dt*) as a function of substrate stiffness. In the first phase of contraction (t <100 s), the rate of force build-up strongly increases for compliant substrates, and presents slight changes for stiffer ones as found by (Mitrossilis et al. 2009) (exp 1 in the legend). (b) Inverse of cell speed of shortening (v_{cell}) as a function of substrate stiffness. The cell contracts faster for softer substrates, v_{cell} approaching zero for K_{subs} >1000 nN/μm. The curve behaves similarly to experiments (Mitrossilis et al. 2009) (c) Normalized mechanical power vs. normalized force. P presents a bi-phasic behaviour with the load, showing a peak at ~40% of the maximum generated force. These behaviors are qualitatively similar to those found by (exp 1, Mitrossilis et al. 2009).

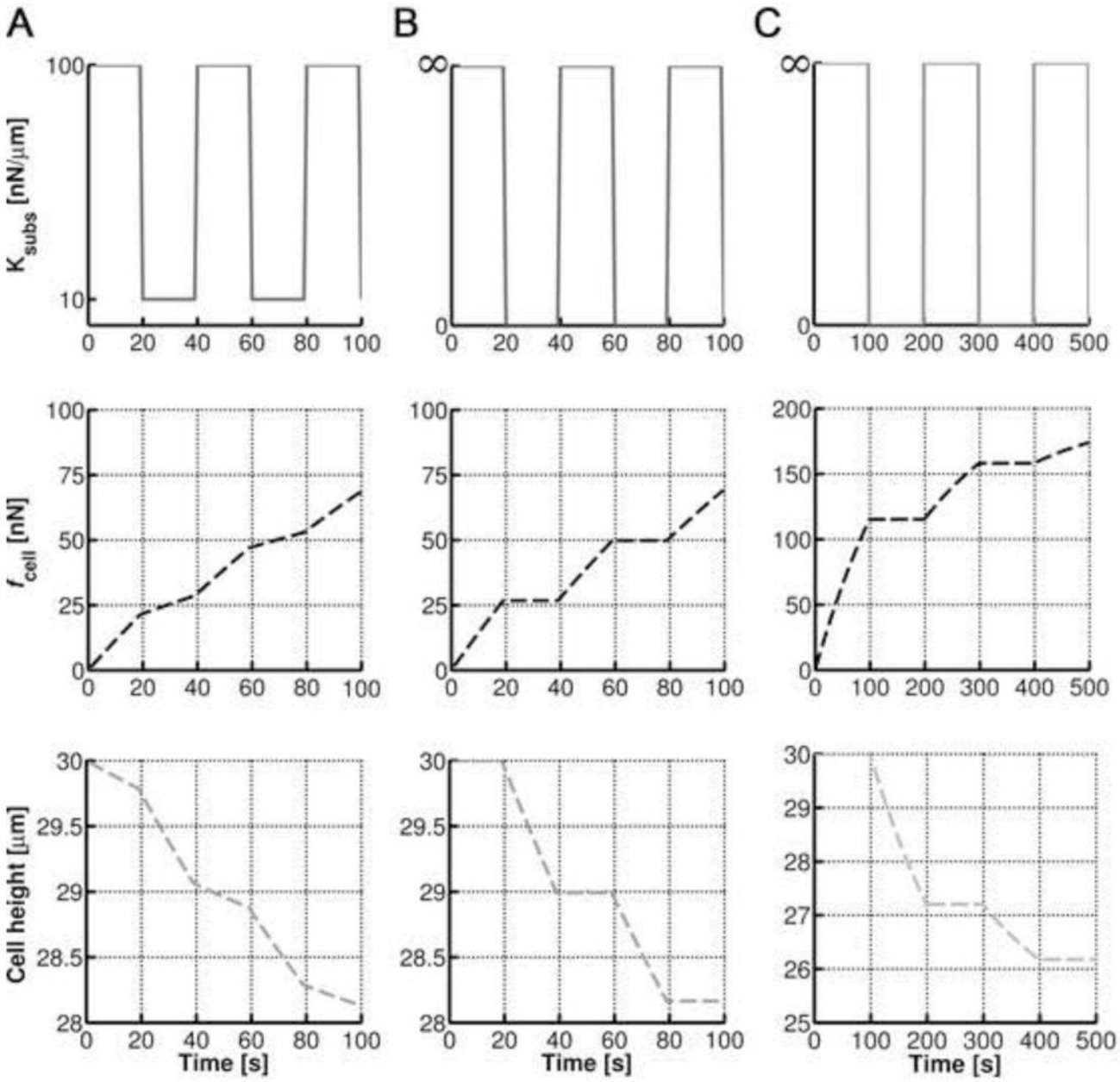

Fig. 6.

Cell response to step-changes in substrate stiffness. (a) The stiffness switches from 10 to 100 nN/μm with a period of 20 seconds to simulate the experiments from (Webster et al. 2011, Crow et al. 2012). The force generated increases faster (higher slope) when the stiffness is higher. The cell height, however, decreases faster for low substrate stiffness. (b) The stiffness switches from 0 to ∞ with periods of 20 seconds (Crow et al. 2012) and (c) 100 seconds (Mitrossilis et al. 2009). The force increases at maximum rate for a completely rigid substrate, whereas the cell height remains invariable. Nevertheless, for a completely compliant substrate, there is no force development and the cell body contracts at maximum speed.

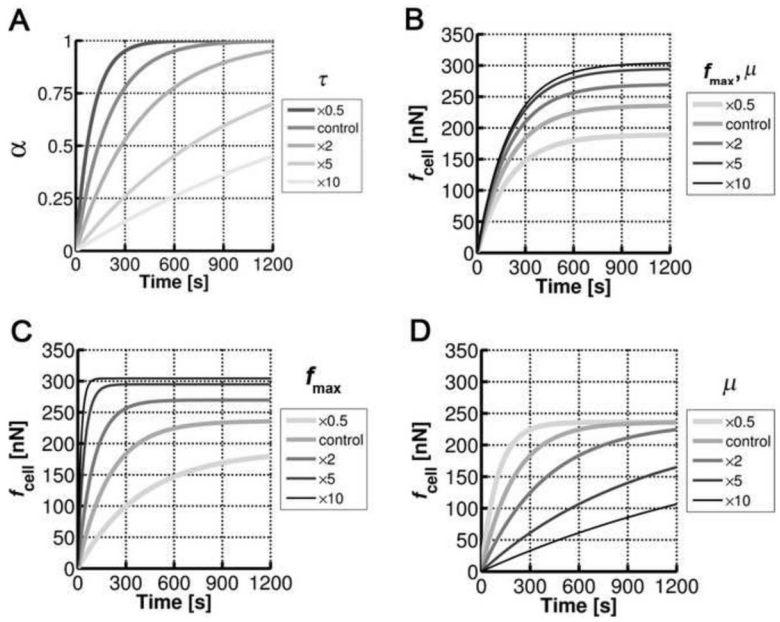

Fig. 7.

Sensitivity analysis of parameters involved in motor stalling evolution (α).(a) Evolution of stalling depending on the relaxation time (τ). For higher values of τ, α needs more time to reach plateau. (b) If f_{max} and μ are varied together, the relaxation time (τ) remains constant, whereas the magnitude of exerted forces changes. (c) f_{max} affects both the relaxation time and the mechanical equilibrium. Higher values of f_{max} correspond with higher plateu forces attained faster. (d) The viscosity coefficient only affects the time-evolution. Thus, changes in μ are equivalent to changes in the relaxation time.

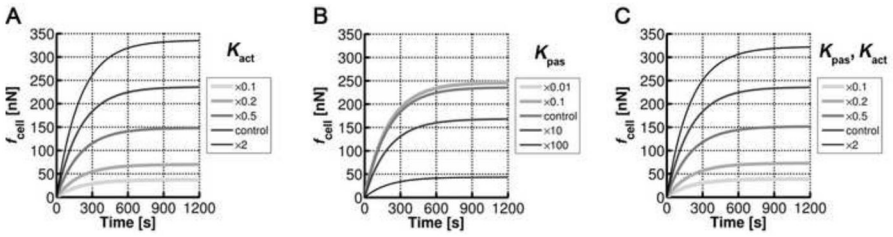

Fig. 8.

Sensitivity analysis of the cell force evolution depending on actin (K_{act}) and passive stiffness (K_{pas}). (a) Changes in K_{act} lead to important changes in the plateau force. High values of actin stiffness decrease the contraction of the AM system, thus producing higher forces. (b) Variations of the cell passive stiffness affect the force generation only when the values of K_{pas} are similar or greater than the values of K_{act}. (c) By varying both K_{act} and K_{pas} at the same time, the changes in force generation are similar to those obtained when varying only K_{act}, confirming that the actin stiffness is the predominant mechanical parameter.

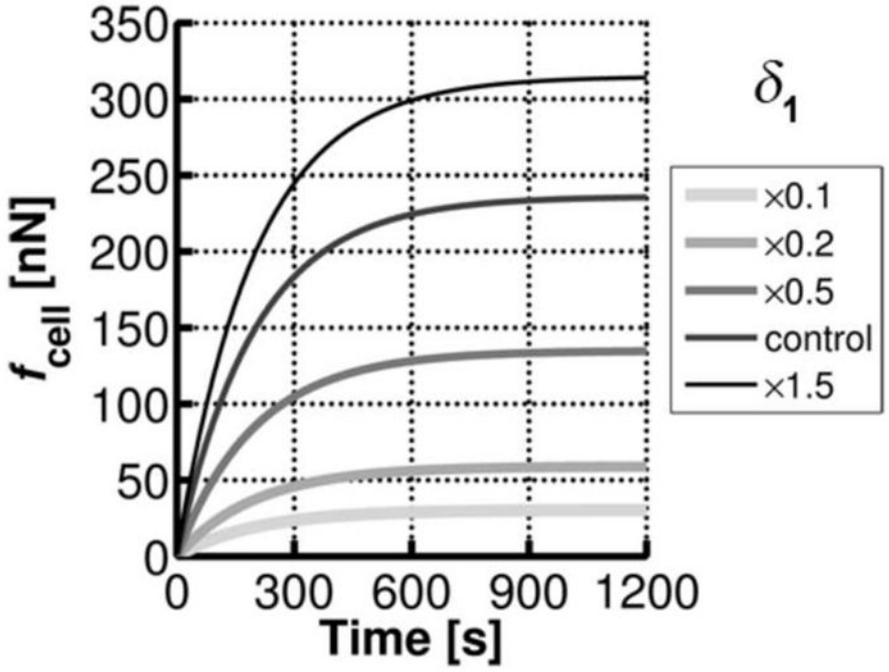

Fig. 9.

Sensitivity analysis of the cell force evolution depending on slippage distance (δ_1) for K_{subs} =100 nN/μm. Higher values of δ_1 enhance system contractility, leading to higher exerted forces.

Table 1

Parameter list

Variable	Symbol	Value	Units	References
Actin stiffness	K_{act}	28	[nN/μm]	(Schafer and Radmacher 2005; Lim et al. 2006)
Passive CSK stiffness	K_{pas}	5.6	[nN/μm]	(Schafer and Radmacher 2005; Lim et al. 2006)
Substrate stiffness	K_{subs}	1–1000	[nN/μm]	(Mitrossilis et al. 2009; Mitrossilis et al. 2010)
Maximum slippage distance	δ_1	−15	[μm]	*
Zero-slippage force	f_{max}	1000	[nN]	(Mitrossilis et al. 2009; Mitrossilis et al. 2010)
Cell length	$Lc_{,0}$	30	[μm]	(Crow et al. 2012)
Viscosity coefficient	μ	$2e^5$	[nN.s]	*
Relaxation time	τ	200	[s]	*

*Adjusted parameters